MOLECULAR AND CELLULAR BIOLOGY, Aug. 2006, p. 6139–6148 Vol. 26, No. 16
0270-7306/06/$08.00+0 doi:10.1128/MCB.00627-06

Lysosomal Phospholipase A2 and Phospholipidosis†

Miki Hiraoka,[1]‡ Akira Abe,[1]‡ Ye Lu,[1] Kui Yang,[2] Xianlin Han,[2] Richard W. Gross,[2] and James A. Shayman[1]*

Nephrology Division, Department of Internal Medicine, University of Michigan, Ann Arbor, Michigan,[1] *and Department of Medicine, Washington University, St. Louis, Missouri*[2]

Received 11 April 2006/Returned for modification 17 May 2006/Accepted 27 May 2006

A lysosomal phospholipase A2, LPLA2, was recently characterized and shown to have substrate specificity for phosphatidylcholine and phosphatidylethanolamine. LPLA2 is ubiquitously expressed but is most highly expressed in alveolar macrophages. Double conditional gene targeting was employed to elucidate the function of LPLA2. LPLA2-deficient mice (*Lpla2*$^{-/-}$) were generated by the systemic deletion of exon 5 of the *Lpla2* gene, which encodes the lipase motif essential for the phospholipase A2 activity. The survival of the *Lpla2*$^{-/-}$ mice was normal. *Lpla2*$^{-/-}$ mouse mating pairs yielded normal litter sizes, indicating that the gene deficiency did not impair fertility or fecundity. Alveolar macrophages from wild-type but not *Lpla2*$^{-/-}$ mice readily degraded radiolabeled phosphatidylcholine. A marked accumulation of phospholipids, in particular phosphatidylethanolamine and phosphatidylcholine, was found in the alveolar macrophages, the peritoneal macrophages, and the spleens of *Lpla2*$^{-/-}$ mice. By 1 year of age, *Lpla2*$^{-/-}$ mice demonstrated marked splenomegaly and increased lung surfactant phospholipid levels. Ultrastructural examination of *Lpla2*$^{-/-}$ mouse alveolar and peritoneal macrophages revealed the appearance of foam cells with lamellar inclusion bodies, a hallmark of cellular phospholipidosis. Thus, a deficiency of lysosomal phospholipase A2 results in foam cell formation, surfactant lipid accumulation, splenomegaly, and phospholipidosis in mice.

Previously, a novel enzyme was discovered in the lysosomal fraction of MDCK cells. The enzyme was characterized as having ceramide transacylase and phospholipase A2 activity (3). The enzyme was purified, cloned, and named lysosomal phospholipase A2 (LPLA2) (12). Characteristics of the enzyme include a pH optimum of 4.5 and calcium independence. In addition, phosphatidylcholine and phosphatidylethanolamine are preferentially favored as substrates for the phospholipase A2. The enzyme is highly homologous with lecithin cholesterol acyltransferase and is phylogenetically related to a large group of plant phospholipases (15). Most recently, the phospholipase activity was demonstrated as highly expressed in alveolar macrophages, suggesting a potential role for LPLA2 in the phospholipid catabolism of pulmonary surfactant (1). LPLA2-deficient mice were generated to further evaluate the biological function of LPLA2.

In the present study, double conditional targeted mice were generated, and the targeted gene was modified using Cre/loxP and Flp/FRT recombination systems. Lpla2-deficient mice were generated in which exon 5 of the *Lpla2* gene, which encodes the lipase motif essential for Lpla2 activity, was systemically deleted. The resultant *Lpla2*$^{-/-}$ mice showed no LPLA2 activity, developed normally, and were characterized by a marked accumulation of phospholipid in their alveolar macrophages, peritoneal macrophages, and spleens at an early age. Increased lung surfactant phospholipid and splenomegaly were observed in mice by 1 year of age.

* Corresponding author. Mailing address: Department of Internal Medicine, University of Michigan, Room 1560 MSRB II, 1150 West Medical Center Dr., Ann Arbor, MI 48103-0676. Phone: (734) 763-0992. Fax: (734) 763-0982. E-mail: jshayman@umich.edu.

† Supplemental material for this article may be found at http://mcb.asm.org/.

‡ These authors contributed equally to this work.

MATERIALS AND METHODS

Reagents. Synthetic phospholipids, including 1,2-dioleloyl-*sn*-glycero-3-phosphorylcholine (DOPC), 1-palmitoyl-2-oleoyl-*sn*-glycero-3-phosphorylcholine (POPC), and 1,2-dimyristoleoyl-*sn*-glycero-3-phosphocholine (14:1-14:1 PC); 1,2-dipentadecanoyl-*sn*-glycero-3-phosphoethanolamine (15:0-15:0 PE); 1,2-dipenta-decanoyl-*sn*-glycero-3-phosphoglycerol (15:0-15:0 PG); 1,2-dimyristoyl-*sn*-glycero-3-phosphoserine (14:0-14:0 PS); 1-heptadecanoyl-2-hydroxyl-*sn*-glycero-3-phos-phocholine (17:0 lysoPC); and *N*-heptadecanoyl ceramide (N17:1 Cer) were purchased from Avanti Polar Lipids, Inc. (Alabaster, AL). Deuterated palmitic acid (d_4-16:0 FA) was purchased from Cambridge Isotope Laboratories (Andover, MA). Dicetyl phosphate was purchased from Sigma (St. Louis, MO), 1-palmitoyl-2-[^{14}C]oleoyl-*sn*-3-glycero-phosphorylcholine (25 μCi/ml) was from Amersham Biosciences (Piscataway, NJ), and *N*-acetyl-D-*erythro*-sphingosine (NAS) was from Matreya (Pleasant Gap, PA). Bicinchoninic acid protein assay reagent was obtained from Pierce Chemical (Rockford, IL).

Generation of *Lpla2* double conditional targeted mice. The genome sequence containing the *Lpla2* gene was obtained from screening the Resgen CJ7 embryonic stem (ES) cell line BAC clone library (Invitrogen, Carlsbad, CA). A SmaI-SacI fragment of approximately 8,450 bp of the *Lpla2* gene was subcloned into the pUC vector. In a previous report it was shown that the lipase motif, located within exon 5, is essential for LPLA2 enzyme activity (12). Therefore, to create the conditional null allele, the SpeI-DraI region containing exon 5 was floxed with two *loxP* sites and then inserted into the vector (Fig. 1A). The PGK-*neo* cassette flanked with two *FRT* sites was inserted at the SpeI site in the intron between exons 4 and 5 in reverse orientation. The targeting vector was sequenced to ensure that no mutation had been introduced and then was linearized by NdeI digestion and electroporated into CJ7 ES cells. Homologous recombinant clones were obtained from G418-resistant colonies screened at a frequency of 20%. The G418-resistant clones were screened by PCR using primers inside and outside the targeting construct. A correctly targeted clone was injected into C57BL/6 blastocysts. The chimeric mice were mated with C57BL/6 to obtain heterozygous mice carrying the targeted allele. Mice carrying the targeted allele were mated with *flp1* mice (stock no. 3800; The Jackson Laboratory) to delete the *neo* cassette. The conditional heterozygous mice were then mated with *EIIa Cre* mice of C57BL/6 background (stock no. 3724; The Jackson Laboratory) to excise the region containing exon 5. The heterozygous mice carrying the null allele were mated to generate homozygous (−/−), heterozygous (+/−), and wild-type (+/+) littermates of the *Lpla2* null allele. Homologous recombination at the null allele was screened by PCR (Fig. 1B). Genomic DNA was extracted from the tails of the mice. The PCR primers were as follows: a, 5′-CAGGGTA GCTCACAACTCTTTG-3′; b, 5′-CAAAGCTCTGGACTGTTTTCCTGC-3′; c,

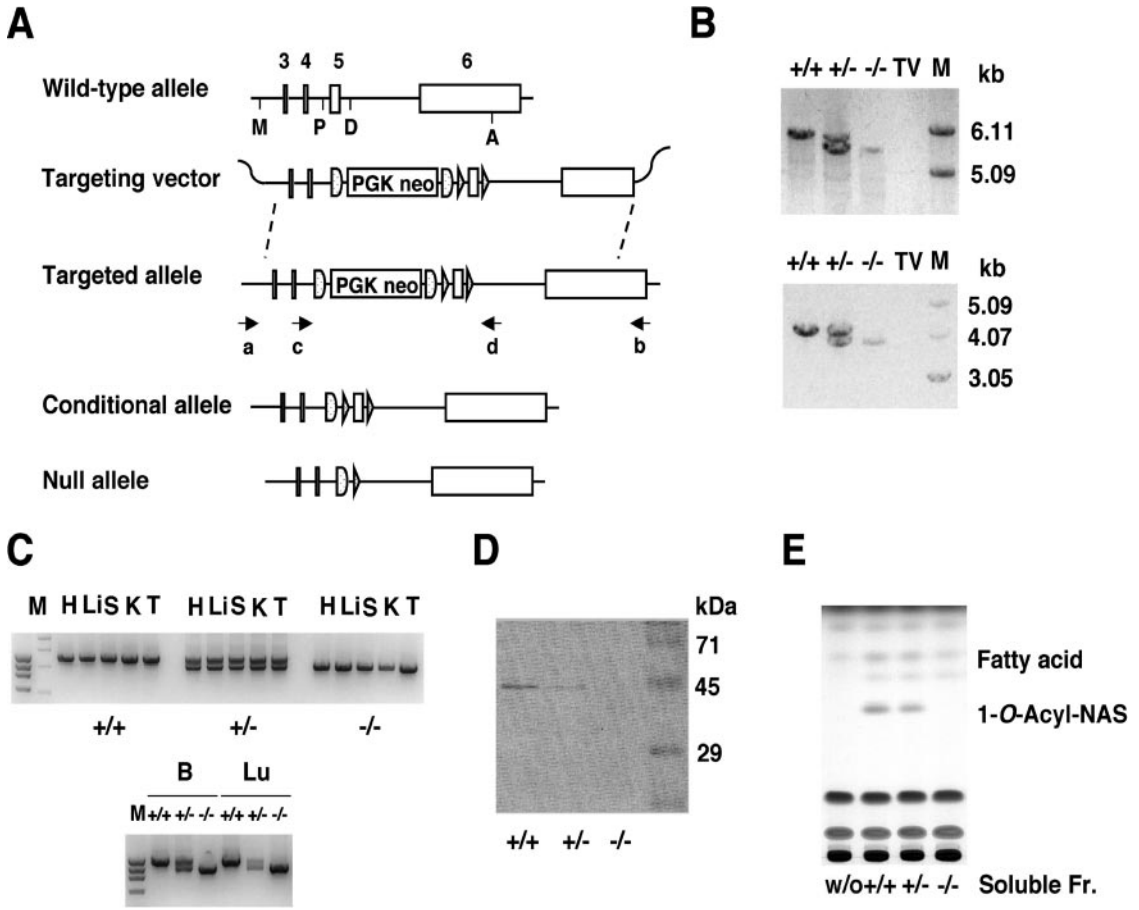

FIG. 1. A. Strategy for producing allelic series of mutations at the Lpla2 locus. The partial map of the murine Lpla2 locus is displayed. Horizontal lines and open boxes with numbers represent introns and Lpla2 exons, respectively. Vertical lines represent restriction sites: M, SmaI; P, SpeI; D, DraI; A, SacI. The Lpla2 double conditional targeting vector was designed. Shaded triangles represent *loxP* sites flanking the *Lpla2* gene exon 5, and shaded half-circles represent FRT sites flanking the neomycin resistance cassette (PGK *neo*). The targeted allele was generated by homologous recombination. The primers used for PCR are shown as horizontal arrows with letters. The conditional allele was generated by Flp-mediated excision. The heterozygous mice carrying targeted alleles were mated with *FLP1* transgenic mice to delete the *neo* cassette. The null allele was generated by Cre-mediated excision. The heterozygous mice carrying conditional alleles were mated with *EIIa Cre* transgenic mice to delete exon 5. B. Genotype analysis by PCR. Genomic DNA was extracted from mouse tail, and PCR was performed to evaluate homologous recombination. The primers a and d as well as b and c were used for upper panel and lower panel assays, respectively. TV indicates targeting vector. M indicates molecular marker. C. Reverse transcription-PCR assay. Total RNAs were isolated from various mouse organs and synthesized cDNA. PCR was performed using primers which are able to cover the Lpla2 coding region. M, molecular marker ϕ_174 RF DNA/HaeIII; H, heart; Li, liver; S, spleen; K, kidney; T, thymus; B, brain; Lu, lung. D. Immunoblots of Lpla2 from the alveolar macrophages obtained from $Lpla2^{+/+}$, $Lpla2^{+/-}$, and $Lpla2^{-/-}$ mice. Alveolar macrophages were isolated from mice as described in Materials and Methods, and the soluble fraction was separated by gel electrophoresis as previously described (1). A rabbit anti-LPLA2 polyclonal antibody (^{100}RTSRATQFPD^{109}) was used for detection. E. Transacylase activity in the soluble fraction of alveolar macrophages obtained from $Lpla2^{+/+}$, $Lpla2^{+/-}$, and $Lpla2^{-/-}$ mice. Each soluble fraction (3 μg of protein) obtained from 3-month-old $Lpla2^{+/+}$, $Lpla2^{+/-}$, and $Lpla2^{-/-}$ mouse alveolar macrophages was incubated for 30 min at 37°C in citrate buffer, pH 4.5, with 40 μM NAS in liposomal form, and formation of 1-*O*-acyl-NAS was determined as described in Materials and Methods. The transacylase specific activities for the $Lpla2^{+/+}$, $Lpla2^{+/-}$, and $Lpla2^{-/-}$ mouse alveolar macrophages were 3.9 μg/min/mg protein, 2.08 μg/min/mg protein, and undetected, respectively. w/o, without; Fr., fraction.

5′-GAATTCCTAGACCCCAGCAAGAAGAATGTG-3′; and d, 5′-CCCTCCC CAGAGATGGATATTT-3′. Primers a and d generated 5.8-kb and 5.5-kb products from a wild-type allele and a null allele by PCR, respectively. Primers b and c generated 4.1-kb and 3.8-kb products from a wild-type allele and a null allele by PCR, respectively. The PCR amplification employed 35 cycles with steps at 94°C for 30 s, 60°C for 30 s, and 72°C for 3 min, which was extended 20 s every cycle for the last 25 cycles using *ExTaq* DNA polymerase (Takara Bio, Shiga, Japan). The PCR products were subjected to electrophoresis, purification, and sequencing. To confirm wild-type, conditional, and null alleles, the PCR with primers c and d using *rTaq* polymerase (Takara Bio) employed 35 cycles with steps at 94°C for 30 s, 60°C for 30 s, and 72°C for 1 min. The product sizes were 1,212, 1,444, and 894 bp for the wild-type, conditional, and null alleles, respectively.

Reverse transcription-PCR analysis. Total RNA was isolated from each mouse organ using Trizol reagent (Invitrogen) followed by purification using an RNeasy kit (QIAGEN, Valencia, CA). The total RNA was used to synthesize cDNA with oligo(dT)$_{12\text{-}18}$ primers in the SuperScript First-Strand synthesis system (Invitrogen). Primers used for PCR were 5′-ATGGATCGCCATCTC-3′ (forward) and 5′-TCAAGGTTCCAGAAGCACACGTTT-3′ (reverse). PCR was performed using *rTaq* polymerase with the conditions described above. PCR products were purified and sequenced.

Isolation of mouse macrophages and tissues. All mice were housed in specific-pathogen-free conditions and used at 2 to 12 months of age. After anesthesia with CO_2 inhalation, the organs were isolated. For isolation of alveolar macrophages, the tracheae were cannulated and the lungs were lavaged with phos-

phate-buffered saline (PBS) containing 0.5 mM EDTA. Peritoneal macrophages were obtained by lavage of the peritoneal spaces with PBS containing 0.5 mM EDTA. After being counted, cells were suspended in RPMI 1640 medium containing 1× antibiotic-antimycotic solution (Invitrogen) and plated in culture dishes, followed by incubation at 37°C in a humidified atmosphere of 5% CO_2 in air. Nonadherent cells were removed by washing with PBS. Under these conditions, the recovered cells were greater than 90% macrophages as measured by Wright-Giemsa and anti-CD68 staining. The University of Michigan Committee on the Use and Care of Animals approved all experiments.

Electron microscopy. Fresh tissue was minced into 1-mm cubes, and alveolar and peritoneal lavage cells were collected and then fixed by immersion in 4% glutaraldehyde, 0.1 M sodium cacodylate buffer (pH 7.3). The sample was post-fixed with osmium tetroxide before embedding in Epon. One-micrometer sections, stained with toluidine blue, were screened by light microscopy to select cross-sections for ultrastructural study. Thin sections were stained with uranyl acetate and lead citrate before examination with a Philips 400T transmission electron microscope. Representative photomicrographs were selected.

Preparation of cell homogenate and soluble fraction from mouse alveolar and peritoneal macrophages and tissues. For the preparation of the soluble fractions of alveolar macrophages and peritoneal macrophages, the cells were allowed to adhere to 35-mm culture dishes, washed three times with 2 ml of cold PBS, scraped with a small volume of PBS, and transferred into 15-ml plastic tubes. The cells were collected by centrifugation at 800 × *g* for 10 min at 4°C and resuspended with 0.4 to 1.0 ml of cold 0.25 M sucrose, 10 mM HEPES (pH 7.4), 1 mM EDTA. The cell suspension was disrupted five times with a probe-type sonicator for 10 s at 0°C to obtain the cellular homogenate. The homogenate was centrifuged for 1 h at 100,000 × *g* at 4°C. The resultant supernatant was passed through a 0.2-μm filter and used as a soluble fraction. For the preparation of soluble fractions of mouse tissues, each organ was washed with cold PBS, weighed, and homogenized by a Potter Elvehjem homogenizer with cold 0.25 M sucrose, 10 mM HEPES (pH 7.4), 1 mM EDTA. The homogenate was centrifuged for 10 min at 600 × *g* at 4°C. The resultant supernatant was sonicated with a probe-type sonicator for 10 s five times at 0°C and centrifuged for 1 h at 100,000 × *g* at 4°C. The supernatant was passed through a 0.2-μm filter and used as a soluble fraction.

Enzyme phospholipase A2/transacylase assay. Phospholipids, DOPC and PE, and *N*-acetylsphingosine were used in the assay system as donor and an acceptor, respectively, of an acyl group. The transacylase activity by LPLA2 was determined by analysis of 1-*O*-acyl-*N*-acetylsphingosine formation rate. The reaction mixture consisted of 45 mM sodium citrate (pH 4.5), 10 μg/ml bovine serum albumin, and 40 μM *N*-acetylsphingosine incorporated into phospholipid liposomes (DOPC/PE/dicetyl phosphate/*N*-acetylsphingosine [5:2:1:2 molar ratio]) and soluble fractions (0.7 to 10 μg) in a total volume of 500 μl. The reaction was initiated by adding the soluble fraction, kept for 5 to 60 min at 37°C, and terminated by adding 3 ml of chloroform/methanol (2:1) plus 0.3 ml of 0.9% (wt/vol) NaCl. The mixture was centrifuged for 5 min at room temperature. The resultant lower layer was transferred into another glass tube and dried under a stream of nitrogen gas. The dried lipid dissolved in 40 μl of chloroform/methanol (2:1) was applied on an high-performance thin-layer chromatography (HPTLC) plate and developed in a solvent system consisting of chloroform/acetic acid (9:1). The plate was dried and soaked in 8% (wt/vol) $CuSO_4$, $5H_2O$, 6.8% (vol/vol) H_3PO_4, 32% (vol/vol) methanol. The wet plate was briefly dried with a hair dryer and charred for 15 min in a 150°C oven. The plate was scanned, and NIH-image 1.62 was used to quantify the reaction products.

The following protocol was used for the phospholipase A2 assay without *N*-acetylsphingosine as an acceptor. The reaction mixture contained 48 mM sodium citrate (pH 4.5), 10 μg/ml bovine serum albumin, liposomes (130 μM phospholipid), and 1.77 μg/ml of the soluble fraction obtained from *Lpla2*$^{+/+}$ or *Lpla2*$^{-/-}$ mouse alveolar macrophages in 500 μl of total volume. The liposomes consisted of 1-oleoyl-2-palmitoyl-*sn*-glycero-3-phosphocholine and dicetylphosphate in the molar ratio 10:1, with a trace of 1-palmitoyl-2-1-[^{14}C]palmitoyl-L-*sn*-glycero-3-phosphocholine (2.8×10^5 cpm/assay). The reaction was initiated by adding 20 μl of each soluble fraction or sucrose buffer, kept for 15, 30, and 45 min at 37°C, and terminated by the addition of 3 ml of chloroform/methanol (2:1) plus 300 μl of 0.9% NaCl. The resultant lower layer was transferred into a small glass tube and dried under a stream of nitrogen gas. The dried lipid was redissolved with chloroform/methanol (2:1) and applied to an HPLTC plate. The plate was developed in a solvent system consisting of chloroform/methanol/pyridine (98:2:0.5). After development, the plate was dried, sprayed with ENHANCE, and exposed on X-ray film at −80°C for 20 h. In the study using lung tissue, the same reaction was initiated by the addition of 10 μg of lung soluble fraction and kept for 30, 60, and 90 min at 37°C.

Lipid analysis. Lipids were extracted from tissues, alveolar macrophages, peritoneal macrophages, and bronchoalveolar lavage fluid of 3-month-old mice by the partially modified method of Bligh and Dyer (5). The phospholipid content was measured by the method of Ames (4). Individual phospholipids were separated by high-performance thin-layer chromatography and quantified as described above. Disaturated phosphatidylcholine in samples was isolated by the method of Mason et al. (13). Whole-lipid extract (20 to 100 nmol as phospholipid) was dried under a stream of nitrogen gas. The dried lipid was dissolved in 500 μl of 6.2 mg/ml osmium tetraoxide in carbon tetrachloride and incubated for 15 min at room temperature. The reaction mixture was dried under a stream of nitrogen gas, redissolved in 500 μl of chloroform/methanol (20:1, vol/vol), and applied to an alumina column (0.6 g of activated neutral aluminum oxide, 150 mesh) preequilibrated with chloroform/methanol (20:1, vol/vol). The column was washed with 8 ml of chloroform/methanol (20:1, vol/vol). Disaturated phosphatidylcholine was eluted with 4 ml of chloroform/methanol/7 M ammonium hydroxide (70:30:2, vol/vol), and the eluted fraction was dried under a stream of nitrogen gas. Phosphate content was determined by the method of Ames (4).

For electrospray ionization/mass spectrometry (ESI/MS), lipid extraction from alveolar macrophage preparations (0.1 to 0.5 mg of proteins) was performed using a modified method of Bligh and Dyer as previously described in detail (11). Briefly, internal standards, including 14:0–14:0 phosphatidylserine (8.0 nmol/mg protein), 15:0-15:0 phosphatidylglycerol (6 nmol/mg protein), 15:0-15:0 PE (13 nmol/mg protein), 14:1-14:1 PC (20 nmol/mg protein), 17:0 lysoPC (2 nmol/mg protein), N17:1 ceramide (0.24 nmol/mg protein), and d_4-16:0 fatty acid (12 nmol/mg protein), were added to each individual sample based on protein concentration. Lipids from each sample were extracted against 2 ml of 50 mM LiCl twice, back extracted against 2 ml of 10 mM LiCl twice, filtered with a 0.2-μm polytetrafluoroethylene syringe filter, and finally stored in chloroform/methanol (1:1, vol/vol) at a concentration of 600 μl/mg protein. The lipid extracts were finally flushed with nitrogen, capped, and stored at −20°C for ESI/MS analyses (typically within 1 week). Each lipid solution was further diluted approximately 10-fold just prior to infusion and lipid analysis. To this diluted lipid solution, LiOH (50 nmol/mg of protein) was added just prior to performing further lipid analyses in both negative- and positive-ion modes.

ESI/MS analyses were performed utilizing a triple-quadrupole mass spectrometer (ThermoElectron TSQ Quantum Ultra, San Jose, CA) equipped with an electrospray ion source as described previously (11). Typically, a 1-min period of signal averaging in the profile mode was employed for each MS spectrum, and a 1- to 2-min period of signal averaging for each MS/MS spectrum was used. Global analyses of lipid extracts were performed by shotgun lipidomics as described previously (9, 10). Quantitation of each individual molecular species of lipid classes were performed using a two-step process, as described in detail previously (8, 9).

Degradation of 1-palmitoyl-2-[^{14}C]oleoyl-*sn*-glycero-3-phosphorylcholine (POPC) by alveolar macrophages. Alveolar macrophages (1.3×10^6 cells) obtained from 3- to 5-month-old *Lpla2*$^{+/+}$ and *Lpla2*$^{-/-}$ mice were seeded into a 35-mm dish containing 2 ml of RPMI 1640 medium (Invitrogen) containing 1× antibiotic-antimycotic and followed by incubation at 37°C in a humidified atmosphere of 5% CO_2 in air. After 90 min, nonadherent cells were removed by washing with PBS. The adherent cells were incubated with 2.1 ml of RPMI 1640 medium containing 320 μM (0.25 μCi/ml) ^{14}C-labeled POPC in liposomes consisting of POPC/dicetyl phosphate (10:1 molar ratio) for 4 h at 37°C. After the incubation, the cells were washed three times with 2 ml of cold PBS and fixed with 1 ml of cold methanol. The fixed cells were scraped and transferred into a glass tube. An additional 1 ml of methanol was used to recover the remaining cells in the dish. The cell suspension was mixed with 1 ml chloroform plus 0.8 ml of 0.9% NaCl and sonicated in a water bath sonicator briefly and kept for 1 h at room temperature. The mixture was centrifuged for 30 min at 2,000 × *g* at room temperature, and the supernatant was transferred into a long glass tube. The supernatant was mixed and vortexed with 3 ml of chloroform plus 0.8 ml of 0.9% NaCl and centrifuged for 5 min at 800 × *g*. The lower layer was washed with 2 ml of methanol plus 1.6 ml of 0.9% NaCl, centrifuged for 5 min at 800 × *g*, and washed again with 2 ml of methanol plus 1.6 ml of water. The resultant lower layer was transferred into another glass tube and dried under a stream of nitrogen gas. The dried lipid was dissolved in 100 μl of chloroform/methanol (2:1, vol/vol). Half of the lipid extract was applied to an HPTLC plate and developed in a solvent system consisting of chloroform/acetic acid (9:1, vol/vol) or chloroform/methanol/water (60:35:8, vol/vol/vol). After development, the plate was dried, sprayed with ENHANCE, and exposed on X-ray film at −80°C for 4 days.

Nucleotide sequence accession number. The genome sequence containing the *Lpla2* gene has been submitted to GenBank under accession number AY179884.

RESULTS

Generation of LPLA2-deficient mice. To create *Lpla2* null mice, a targeting vector was designed and constructed containing two *loxP* sites and two FRT sites with a PGK-*neo* cassette placed between the FRT sites for modification by use of Cre/loxP and Flp/FRT recombination systems (Fig. 1A). Exon 5, which encodes the lipase motif essential for Lpla2 activity, was floxed with two *loxP* sites and then inserted into the vector. CJ7 ES cells were electroporated with the linearized targeting vector. Homologous recombinant clones were obtained from G418-resistant colonies screened at a frequency of 20%. A correctly targeted clone was injected into C57BL/6 blastocysts. The chimeric mice were mated with C57BL/6 mice to obtain heterozygous mice carrying the targeted allele.

Mice carrying the targeted allele were found to be normal and fertile. However, homozygous offspring from heterozygous pairs showed a modest reduction of Lpla2 activity in the soluble fraction of brain (data not shown). This finding suggested that the *neo* cassette inclusion affected Lpla2 expression. *flp1* transgenic mice express FLP recombinase in the early embryo under the control of the human β-actin promoter. Mice with the targeted allele were mated with *flp1* transgenic mice to delete the *neo* cassette. The allele in which the *neo* cassette was deleted by using an Flp/FRT recombination system is termed the "conditional allele." Mice carrying the conditional allele were normal in appearance and were fertile. The Lpla2 enzyme activity in the homozygous mice carrying the conditional allele was found to be the same as that of wild-type mice (data not shown). *EIIa Cre* transgenic mice express Cre recombinase in the one-cell zygote stage of embryo development under the control of the adenovirus EIIa promoter. Heterozygous mice carrying the conditional allele were mated with *EIIa Cre* transgenic mice to excise the region containing exon 5. The resultant heterozygous mice carrying the null allele were mated together to generate $Lpla2^{-/-}$, $Lpla2^{+/-}$, and $Lpla2^{+/+}$ littermates. Homologous recombination at the null allele was screened by PCR (Fig. 1B). The predicted product from the deletion of the *loxP* site flanking region was detected in both $Lpla2^{-/-}$ and $Lpla2^{+/-}$ but not in the $Lpla2^{+/+}$ mice.

$Lpla2^{+/-}$ mice were viable and fertile. They produced an average of 8.7 pups per litter with a normal Mendelian frequency, indicating no selective fetal or neonatal loss of homozygous pups. Survival of the $Lpla2^{-/-}$ mice was normal. $Lpla2^{-/-}$ mating pairs gave normal litter sizes (8.5 pups per litter), indicating that the gene deficiency did not grossly impair fertility or fecundity. Screening of Lpla2 mRNA expression in seven organs from $Lpla2^{-/-}$ mice demonstrated the deletion of exon 5 in each organ (Fig. 1C), indicating that the deletion was systemic.

An immunoblot was performed on the protein extracts from alveolar macrophages of $Lpla2^{-/-}$, $Lpla2^{+/-}$, and $Lpla2^{+/+}$ mice using a previously generated rabbit polyclonal antibody raised to mouse Lpla2 peptide (^{100}RTSRATQFPD^{109}) (1). A single band at a molecular mass of ca. 44 kDa was observed in blots from $Lpla2^{+/+}$ and $Lpla2^{+/-}$ macrophages. However, no protein was detected from $Lpla2^{-/-}$ alveolar macrophages (Fig. 1D). The Lpla2 enzyme activities were also compared among genotypes. The transacylase activity, as measured by the formation of 1-*O*-acyl-*N*-acetylsphingosine, was absent in $Lpla2^{-/-}$ mouse alveolar macrophages (Fig. 1E). The transacylase activity from $Lpla2^{+/-}$ mouse alveolar macrophages was approximately 50% of that of the $Lpla2^{+/+}$ mouse alveolar macrophages. The deficiency of the enzyme activity in the soluble fraction of the $Lpla2^{-/-}$ mouse was also observed in other cells and tissues, including peritoneal macrophages, heart, lung, liver, spleen, kidney, thymus, and brain (data not shown).

Phospholipid degradation in alveolar macrophages. Many classes of phospholipase A2 exist (17). On the one hand, the absence of ceramide transacylase activity in alveolar macrophages might not necessarily mean that cellular phospholipase A2 activity would be impaired as well. On the other hand, Lpla2 is very highly expressed in alveolar macrophages and might represent the major phospholipase A2 activity. Therefore, the degradation of PC was more extensively evaluated in the mouse alveolar macrophages. A choice of substrate was required. When previously studied, Lpla2 was observed to recognize 1,2-dipalmitoyl-*sn*-glycero-3-phosphorylcholine (DPPC), a major component of pulmonary surfactant lipid, when presented as a substrate in DOPC/DPPC liposomes (1). However, Lpla2 demonstrated greater activity toward DOPC than DPPC. Furthermore, DPPC led to a reduction of the enzyme activity on DOPC in DOPC/DPPC liposomes. These results suggested that unsaturated phospholipids are better substrates than saturated phospholipids and may provide a preferable environment in the Lpla2 reaction.

The transfer of oleic acid to *N*-acetyl-sphingosine and the release of oleic acid from POPC by the soluble fraction obtained from $Lpla2^{+/+}$ mouse alveolar macrophages were observed when POPC/dicetyl phosphate/*N*-acetyl-sphingosine liposomes were used (Fig. 2A). The transacylase activity in the POPC liposome system was comparable to that observed with the DOPC/dicetyl phosphate/*N*-acetyl-sphingosine liposome system. These results were further evaluated with the use of alveolar macrophages and radiolabeled POPC. Using 1-palmitoyl-2-[^{14}C]oleoyl-*sn*-glycero-3-phosphorylcholine, the phospholipase A2 activity was compared between the lungs and alveolar macrophages of $Lpla2^{+/+}$ and $Lpla2^{-/-}$ mice (Fig. 2B). When assayed at pH 4.5, the phospholipase A2 activity in the wild-type lung was 1.10 nmol/min/mg protein but was only 0.072 nmol/min/mg protein in the Lpla2 null mice. The alveolar macrophage activity was 18.6 nmol/min/mg protein versus 0.43 nmol/min/mg protein in the wild-type and knockout mice, respectively. The higher specific activity of Lpla2 in the alveolar macrophages compared to that of the whole lung is consistent with the prior observation reported for Lpla2 assayed as ceramide transacylation (1).

The products of the phospholipase A2 reaction were further evaluated. The radioactive oleic acid released from POPC was readily detected in the lipid extract obtained from the $Lpla2^{+/+}$ mouse alveolar macrophages treated with 1-palmitoyl-2-[^{14}C]oleoyl-*sn*-glycero-3-phosphorylcholine/dicethyl phosphate liposomes (Fig. 2C). On the contrary, there was no radioactive oleic acid detected in the lipid extract obtained from the $Lpla2^{-/-}$ mouse alveolar macrophages treated with ^{14}C-labeled POPC liposomes. The total radioactivity found in the lipid extract, obtained from the $Lpla2^{-/-}$ mouse alveolar macrophages, was approximately one-half of the amount from the $Lpla2^{+/+}$ mouse macrophages. The radioactivity of oleic acid

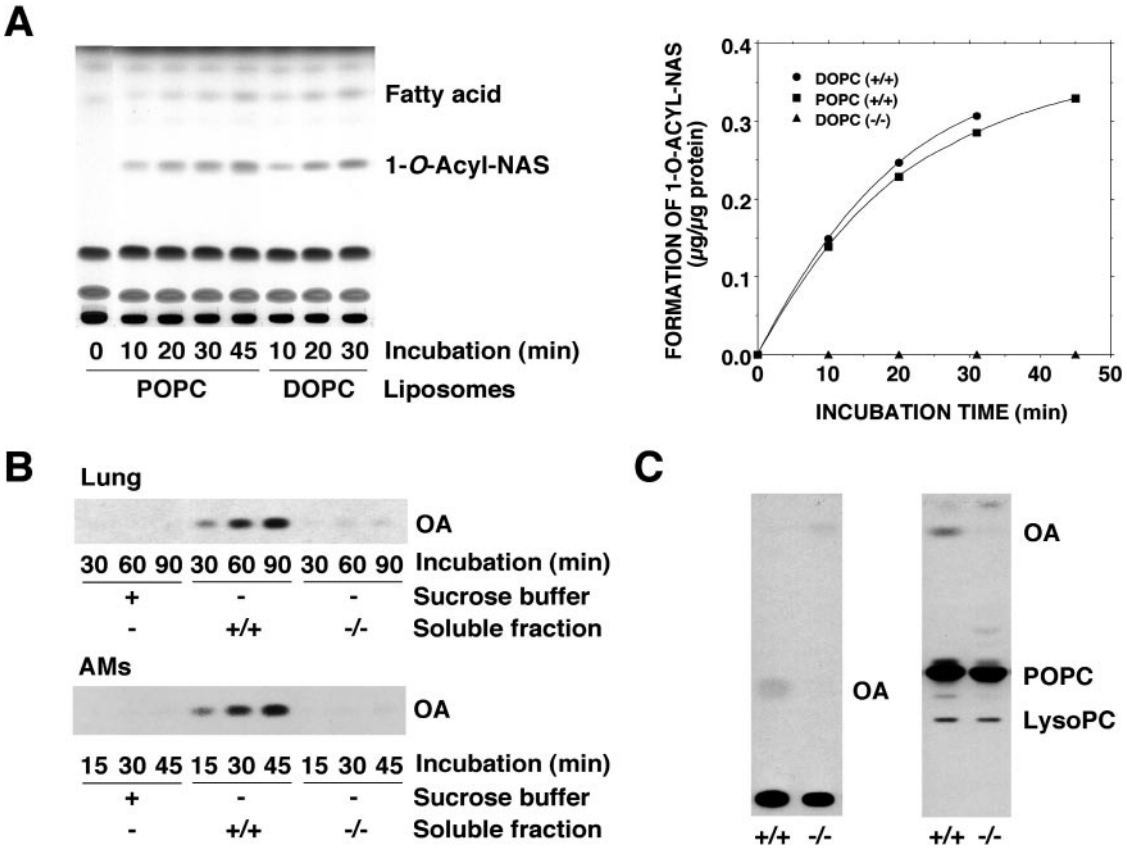

FIG. 2. Lpla2 activities on unsaturated phosphatidylcholines by $Lpla2^{+/+}$ and $Lpla2^{-/-}$ mice. A. Transacylase activities of Lpla2 on two different phosphatidylcholines. The soluble fraction (2 μg of protein) obtained from 3-month-old $Lpla2^{+/+}$ mice was incubated for a suitable time period at 37°C in citrate buffer, pH 4.5, with 40 μM NAS incorporated into phospholipid liposomes (DOPC or POPC/dicetyl phosphate/NAS [7:1:2 molar ratio]), and formation of 1-*O*-oleoyl-NAS was determined as described in Materials and Methods. The left panel shows the TLC. The time-dependent formation of 1-*O*-oleoyl-NAS from DOPC or POPC/dicetyl phosphate/NAS liposomes by the soluble fraction in $Lpla2^{+/+}$ and $Lpla2^{-/-}$ mice. The experiment is representative of three experiments with comparable results. (B) Comparison of phospholipase A2 activities in the lungs and alveolar macrophages of $Lpla2^{+/+}$ and $Lpla2^{-/-}$ mice. Phospholipase A2 activities were measured as described in Materials and Methods using 1-palmitoyl-2-[^{14}C]oleoyl-*sn*-glycero-3-phosphorylcholine. OA denotes oleic acid. C. Degradation of 1-palmitoyl-2-[^{14}C]oleoyl-*sn*-glycero-3-phosphorylcholine by alveolar macrophages. Alveolar macrophages (1.3×10^6 cells) obtained from 3-month-old $Lpla2^{+/+}$ and $Lpla2^{-/-}$ mice were incubated with ^{14}C-labeled POPC/dicetyl phosphate (10:1 molar ratio) liposomes for 4 h at 37°C. After the incubation, the cellular lipid was extracted as described in Materials and Methods. Lipid extract was applied to an HPTLC and developed in a solvent system consisting of chloroform/acetic acid (9:1) (left) or chloroform/methanol/water (60:35:8) (right). After the development, the plate sprayed with ENHANCE was exposed on an X-ray film at −80°C. LysoPC indicates lysophosphatidylcholine. AMs, alveolar macrophages.

recovered from the TLC plate was 260 cpm and 50 cpm for $Lpla2^{+/+}$ and $Lpla2^{-/-}$ mouse macrophages, respectively (Fig. 2C). Additionally, the released radioactive oleic acid was comparably low (40 cpm on the TLC plate) when the ^{14}C-labeled POPC liposomes were incubated with the cultured medium without alveolar macrophages. Thus, 10 times less radioactive oleic acid was released from the $Lpla2^{-/-}$ mouse alveolar macrophages compared to that released from the $Lpla2^{+/+}$ mouse macrophages. Therefore, most of the oleic acid released from POPC in the $Lpla2^{+/+}$ mouse alveolar macrophages was due to Lpla2 activity and not an alternative phospholipase A2.

Interestingly, the radioactive lysoPC was detected in $Lpla2^{+/+}$ and $Lpla2^{-/-}$ alveolar macrophages. This metabolite, labeled in the *sn*-2 position, is produced by phospholipase A1. The radioactivity of lysoPC was 150 cpm and 100 cpm, respectively, for $Lpla2^{+/+}$ and $Lpla2^{-/-}$ mouse alveolar macrophages. These results indicate that the degradation of phospholipid in $Lpla2^{-/-}$ mouse alveolar macrophages is most greatly impaired due to a lack of phospholipase A2 activity.

Phospholipid accumulation in the $Lpla2^{-/-}$ mouse. The phospholipid content and profile in alveolar and peritoneal macrophages and other tissues of 3-month-old $Lpla2^{+/+}$ and $Lpla2^{-/-}$ mice were next examined. The total phospholipid content of the $Lpla2^{-/-}$ mouse alveolar macrophages was more than two times higher than that of the $Lpla2^{+/+}$ mouse alveolar macrophages. Thin-layer chromatography of the lipid extract of the alveolar macrophages showed a marked accumulation of both PE and PC in the $Lpla2^{-/-}$ mouse (see the supplemental material). PE and PC levels were four times and two times higher by scanning in the $Lpla2^{-/-}$ versus $Lpla2^{+/+}$ mouse cells, respectively. Phosphatidylserine, phosphatidylinositol, and sphingomyelin levels were no different, consistent with the known specificity of Lpla2 for PC and PE. The total phospholipid content in the $Lpla2^{-/-}$ peritoneal macrophages

TABLE 1. ESI/MS analysis of alveolar macrophage lipids from 1-year-old mice

Lipid	Lipid level[a] (nmol/mg protein) by phenotype	
	Lpla2$^{+/+}$	Lpla2$^{-/-}$
Phosphatidylcholine	283	538
16:0 Phosphatidylcholine[b]	184	374
Lysophosphatidylcholine	1.2	2.3
Phosphatidylethanolamine	250	524
Plasmalogen phosphatidylethanolamine[c]	173	414
Sphingomyelin	87.4	76.0
Phosphatidic acid	0.74	0.26
Phosphatidylglycerol	79.8	129.0
Ceramide	1.87	2.24
Free fatty acid	124	155

[a] Lipid levels are derived from pooled samples of six mice (three male and three female) from each group. 16:0 designates the presence of palmitoyl containing phosphatidylcholine.
[b] Percent 16:0 PC for Lpla2$^{+/+}$ mice, 65.0; for Lpla2$^{-/-}$ mice, 69.6.
[c] Percent plasmalogen phosphatidyl-ethanolamine for Lpla2$^{+/+}$ mice, 69.2; for Lpla2$^{-/-}$ mice, 78.9.

(305 nmol of phospholipid/mg of protein) was 40% higher than that of the *Lpla2*$^{+/+}$ peritoneal macrophages (223 nmol of phospholipid/mg of protein). A similar change in phospholipid profile was observed in the *Lpla2*$^{-/-}$ peritoneal macrophages.

ESI/MS analysis was used to quantify the lipid content of the *Lpla2*$^{+/+}$ and *Lpla2*$^{-/-}$ alveolar macrophages. Alveolar macrophages were isolated from 12-month-old mice, and internal standards consisting of 14:0-14:0 phosphatidylserine, 15:0-15:0 phosphatidylglycerol, 15:0-15:0 phosphatidylethanolamine, 14:1-14:1 phosphatidylcholine, 17:0 lysophosphatidylcholine, N17:1 ceramide, and d_4-16:0 fatty acid were added to each individual sample based on protein concentration. Marked increases in PC and PE were detected in the null mouse macrophages (Table 1; also see the supplemental material). By contrast, no increase in sphingomyelin or phosphatidic acid was measured. Lysophosphatidylcholine content increased in the null mouse macrophages. However, the total lysophosphatidylcholine concentration was less than 1% of that of phosphatidylcholine. In wild-type mouse macrophages, 65% of the phosphatidylcholine had one or more fatty acids consisting of the 16:0 palmitic acid. Null mice demonstrated a fractional accumulation of saturated species of PC that was proportionate to that found in the wild-type cells (see the supplemental material). These data are consistent with the recognition of saturated species of phosphatidylcholine by Lpla2.

Histologic analysis of alveolar and peritoneal macrophages. Histology was obtained on the lung and major organs of 1-year-old wild-type and null mice. Two marked changes were observed by light microscopy of the lungs. First, alveolar macrophages were present in greater numbers and were larger in size. Second, a mononuclear cell infiltrate was observed in association with both airways and blood vessels (Fig. 3A and B).

Electron microscopy was performed on alveolar and peritoneal macrophages obtained from 3-month-old *Lpla2*$^{-/-}$ and *Lpla2*$^{+/+}$ mice to confirm the presence of phospholipidosis. The alveolar macrophages from the *Lpla2*$^{-/-}$ mice were markedly larger than those from the *Lpla2*$^{+/+}$ mice. Numerous lamellar inclusion bodies, indicative of cellular phospholipidosis, were observed in the *Lpla2*$^{-/-}$ mouse alveolar macrophages (Fig. 4B). However, such lamellar inclusion bodies were only rarely present in the *Lpla2*$^{+/+}$ cells (Fig. 4A). A similar but less robust change was also observed in the peritoneal macrophages (Fig. 4C and 4D). The increase in phospholipid accumulation corresponds to the presence of lamellar inclusions and cellular phospholipidosis.

The phospholipid content of the mouse lung and lavage fluid was measured to ascertain if the development of alveolar foam cells was associated with an increase in total phospholipid content (Table 2). No significant change in total lung phospholipid content was observed in *Lpla2*$^{-/-}$ and *Lpla2*$^{+/+}$ 4-month-old mice. However, significant increases in both lung and lavage fluid phospholipid levels was seen in 12-month-old mice (Table 2). When the levels of disaturated PC content were measured, an increase that was proportionate to total phospholipid levels was observed in both the *Lpla2*$^{-/-}$ mouse lung and lavage fluid.

There was no significant difference in body and organ weights between the *Lpla2* genotypes at 4 months of age. A routine histological survey of their organs, including the hearts, livers, kidneys, brains, and spleen, by hematoxylin and eosin staining showed no gross differences between wild-type and homozygous mice at 4 and 12 months of age (data not shown). However, periodic acid-schiff staining of the organs revealed the presence of foam cells throughout these organs in the homozygous null mice that was most apparent in the spleens of the 1-year-old mice (Fig. 3C and D). By 12 months of age, however, significant splenomegaly was observed in the *Lpla2*$^{-/-}$ mice (Fig. 5A). A greater than fourfold increase in spleen weight was observed. Phospholipid analysis revealed that the increase in phospholipid was primarily due to changes in phosphatidylcholine and phosphatidylethanolamine, consistent with the known substrate specificity of LPLA2 (Fig. 5B and C).

DISCUSSION

We successfully generated *Lpla2*$^{-/-}$ mice using a double conditional targeting system. *Lpla2*$^{-/-}$ mice generated by the systemic deletion of exon 5 of the *Lpla2* gene, which encodes the lipase motif essential for lysosomal phospholipase A2 activity, were healthy at birth and fertile. *Lpla2*$^{-/-}$ mice showed no systemic lysosomal phospholipase A2 activity and a characteristic accumulation of PE and PC in alveolar macrophages, peritoneal macrophages, and spleen. A similar trend in the phospholipid profile was also observed in tissues such as liver and lung but with less accumulation. The selective accumulation of PE and PC in *Lpla2*$^{-/-}$ mice is consistent with the previously reported substrate specificity of Lpla2. Both phospholipids are preferred substrates of Lpla2 (2). Electron microscopy revealed the presence of excessive lamellar inclusion bodies in *Lpla2*$^{-/-}$ alveolar and peritoneal macrophages. This foam cell phenotype is characteristic of cellular phospholipidosis (6).

Phospholipidosis is a generalized condition observed in both animals and humans that is characterized by the appearance of

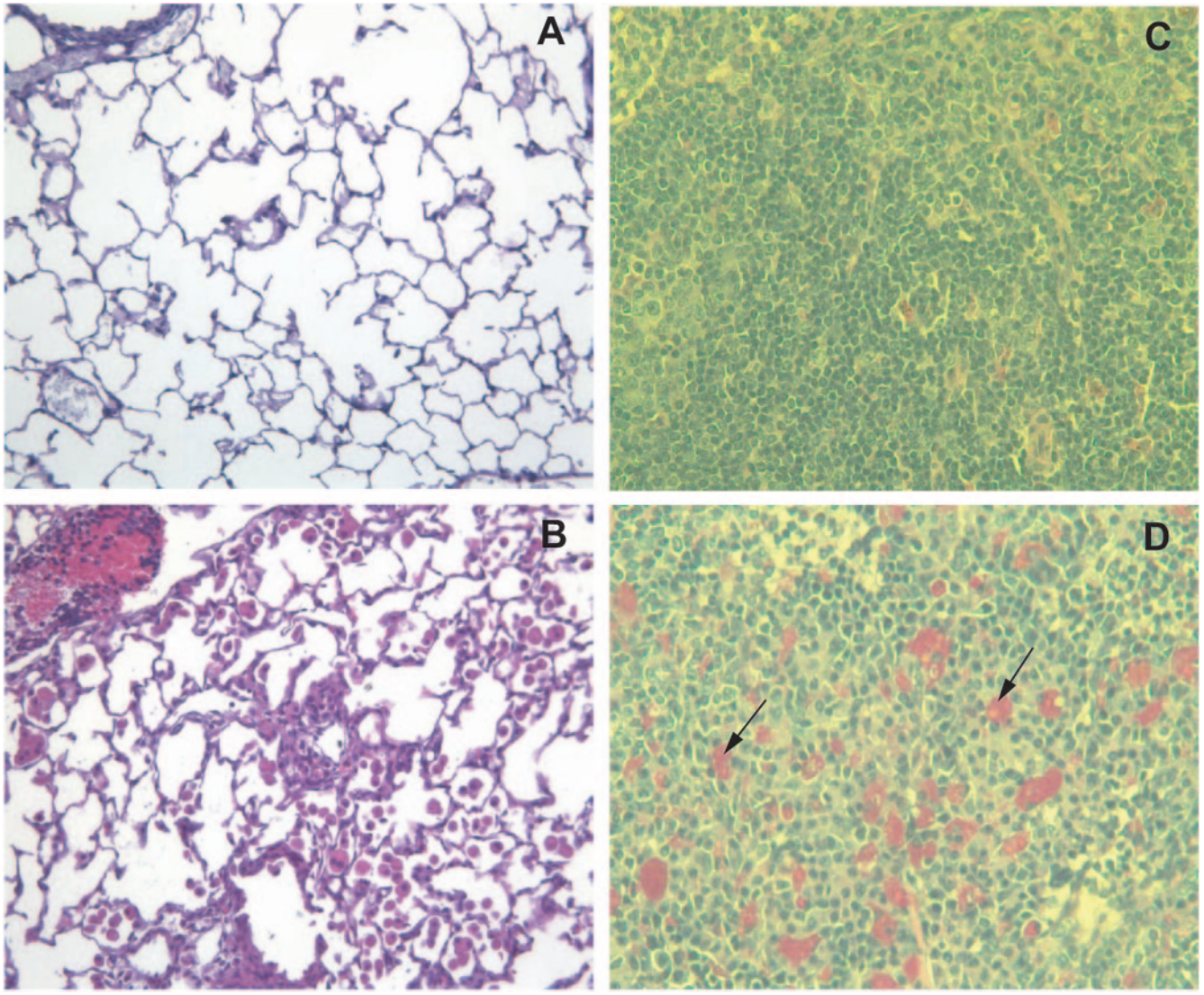

FIG. 3. Light microscopy of tissues from 1-year-old *Lpla2*$^{+/+}$ and *Lpla2*$^{-/-}$ mice. Panels A and B represent PAS staining of formalin-fixed inflated lungs and of spleens from 1-year-old wild-type and *Lpla2*$^{-/-}$ mice, respectively. The histology is noteworthy for increased numbers of enlarged alveolar macrophages, as denoted by the arrows in the air spaces of the null mice and a mononuclear infiltrate surrounding the small airways and arteries. Panels C and D represent PAS staining from the spleens of 1-year-old wild-type and *Lpla2*$^{-/-}$ mice, respectively. PAS-positive macrophages are denoted by the arrows.

concentric lamellar bodies within cells and the intralysosomal accumulation of phospholipids. Phospholipidosis occurs in a variety of clinical settings. Phospholipidosis may be associated with the exposure to xenobiotics. Drugs and their metabolites that induce cellular phospholipid accumulation fall into many different classes, including antiarrhythmics, antipsychotics, antibiotics, and cholesterol-lowering agents. However, these drugs share a common physiochemical structure that includes a hydrophobic ring structure and hydrophilic side chain with a charged cationic amine group (7). Phospholipidosis may also occur in response to environmental exposures such as silica (14). Finally, phospholipidosis is often used synonymously with the term pulmonary alveolar proteinosis to describe the congenital or acquired disease associated with impaired surfactant catabolism (18). Patients suffering from pulmonary alveolar proteinosis present differently from those with drug-induced phospholipidosis. Pulmonary alveolar proteinosis is characterized by a marked accumulation of surfactant lipid; drug-induced phospholipidosis is characterized by secondary inflammatory changes and long-term fibrosis. The consequences of chronic exposure to cationic amphiphilic drugs are poorly understood, in large part due to the absence of a suitable animal model for long-term evaluation (16). In particular, the relationship between the short-term development of lysosomal phospholipid accumulation and long-term inflammation and fibrosis has not been well studied. The Lpla2 knockout mouse is a potentially useful model for elucidating this relationship.

Pulmonary alveolar proteinosis may also be associated with the absence of functional surfactant protein B or loss of granulocyte-macrophage colony-stimulating factor (GM-CSF) ac-

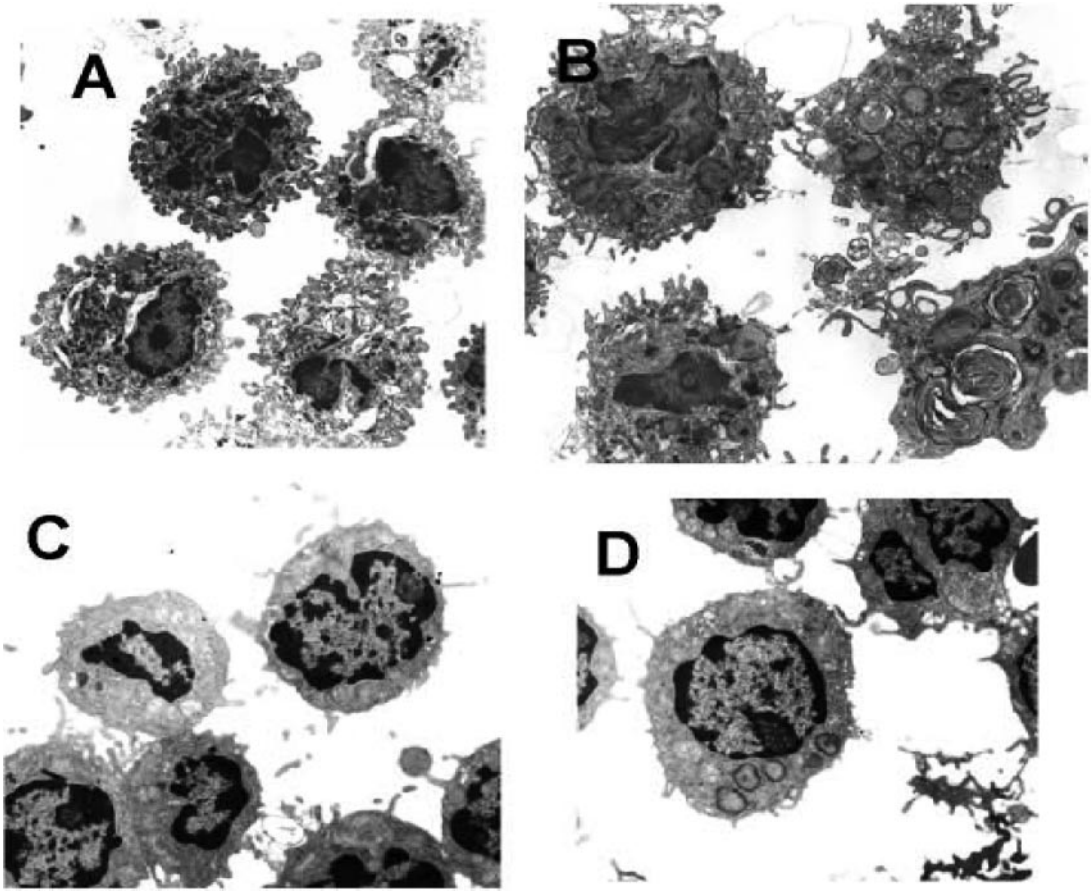

FIG. 4. Electron micrographs of alveolar macrophages (A and B) and peritoneal macrophages (C and D) obtained from 3-month-old *Lpla2*$^{+/+}$ and *Lpla2*$^{-/-}$ mice. (A and C) *Lpla2*$^{+/+}$ mice; (B and D) *Lpla2*$^{-/-}$ mice.

tivity (18). Although the latter is an important factor in alveolar macrophage differentiation, the relationship between loss of GM-CSF and impaired catabolism of surfactant phospholipids is not well understood. Three histological features are observed in the lungs of the GM-CSF knockout mouse. These include the accumulation of surfactant in the airspaces, the development of a foam cell phenotype by alveolar macrophages, and a peribronchial and perivascular inflammation. Two of these findings, the foam cell phenotype and inflammation, are prominently found in the *Lpla2*$^{-}$/$^{-}$ mouse. Although increased surfactant phospholipid could be detected in 1-year-old *Lpla2*$^{-/-}$ mice, this was less robust a finding than that observed in the GM-CSF knockout mouse. In prior work where Lpla2 was found to be highly expressed in alveolar macrophages, the GM-CSF knockout mouse was found to have limited expression of Lpla2, and a GM-CSF transgenic mouse was found to have increased expression of Lpla2 (1). The present study is also consistent with the possibility that Lpla2 mediates at least some of the GM-CSF-dependent changes observed in the lung.

TABLE 2. Protein and phospholipid content of *Lpla2*$^{-/-}$ and *Lpla2*$^{+/+}$ mouse lung and bronchoalveolar lavage fluid

Measurement	*Lpla2*$^{+/+}$	*Lpla2*$^{-/-}$[a]
Total protein (mg/kg of mouse wt)		
Tissue	448.2 ± 12.9	525.9 ± 52.8*
Lavage fluid	16.4 ± 2.6	16.1 ± 7.5
Total phospholipid (μmol/kg mouse wt)		
Tissue	118.9 ± 8.8	155.4 ± 14.9*
Lavage fluid	16.2 ± 1.5	21.6 ± 1.2**
Total disaturated PC (μmol/kg mouse wt)		
Tissue	22.7 ± 2.2	35.4 ± 3.3**
Lavage fluid	8.3 ± 0.7	11.2 ± 0.7**
Total	31.0 ± 2.9	46.6 ± 4.0**

[a] * and ** denote $P < 0.05$ and $P < 0.005$, respectively ($n = 4$).

An additional finding, not reported in the GM-CSF knockout mouse, was the presence of splenomegaly. This finding is consistent with that observed in another disorder of foam cell formation, Gaucher disease. The basis for the splenomegaly is unknown, but in a manner similar to Gaucher disease, it appears to be the result of secondary growth and not from the increase in lipid mass per se. Like Gaucher disease, this finding may be reflective of the role of the splenic macrophage in the clearance of senescent erythrocytes. The Lpla2 null mouse may

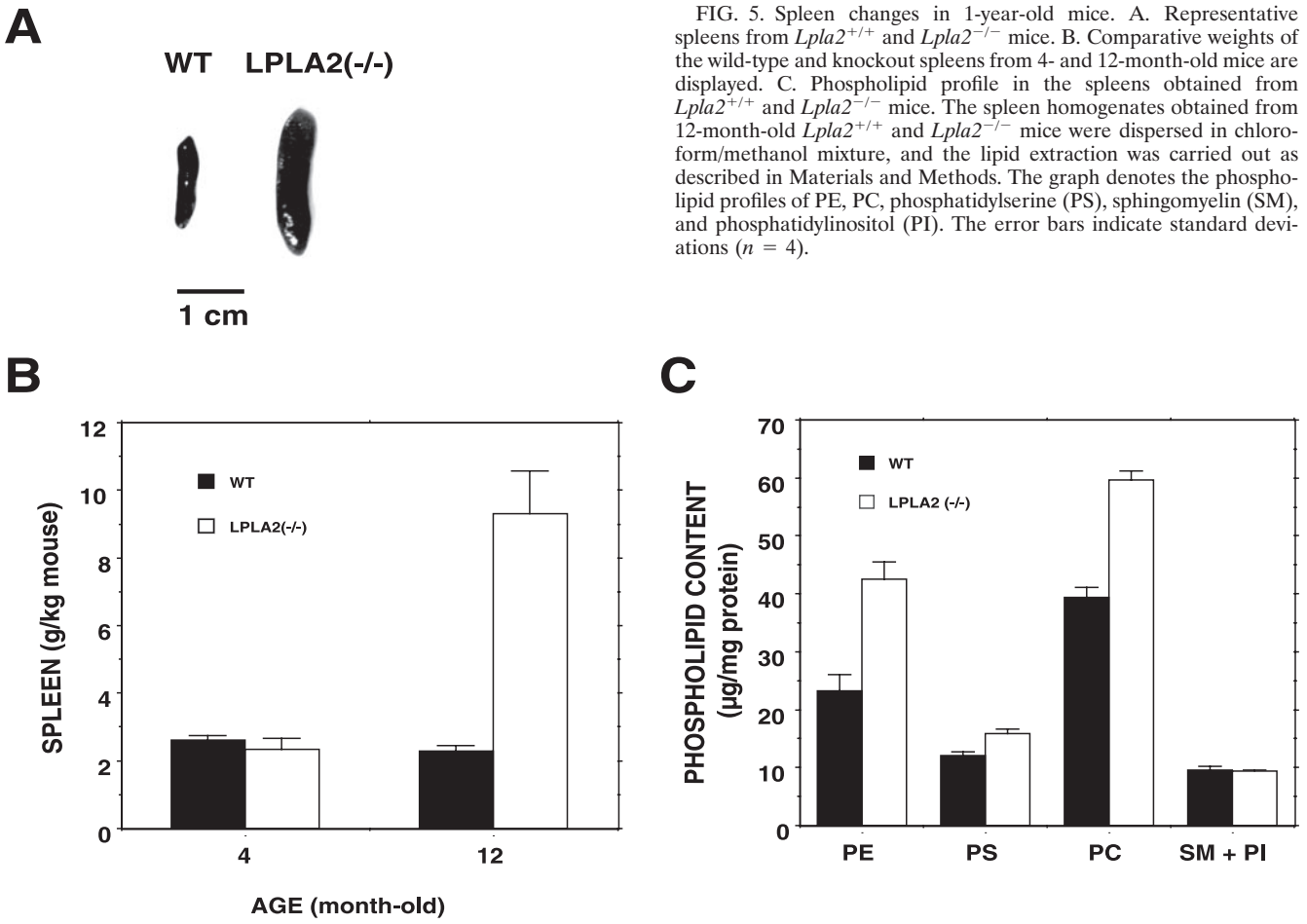

FIG. 5. Spleen changes in 1-year-old mice. A. Representative spleens from *Lpla2*$^{+/+}$ and *Lpla2*$^{-/-}$ mice. B. Comparative weights of the wild-type and knockout spleens from 4- and 12-month-old mice are displayed. C. Phospholipid profile in the spleens obtained from *Lpla2*$^{+/+}$ and *Lpla2*$^{-/-}$ mice. The spleen homogenates obtained from 12-month-old *Lpla2*$^{+/+}$ and *Lpla2*$^{-/-}$ mice were dispersed in chloroform/methanol mixture, and the lipid extraction was carried out as described in Materials and Methods. The graph denotes the phospholipid profiles of PE, PC, phosphatidylserine (PS), sphingomyelin (SM), and phosphatidylinositol (PI). The error bars indicate standard deviations ($n = 4$).

be a useful tool for probing the mechanism behind the lipid-induced organomegaly.

In addition to the increased accumulation of surfactant phospholipid in 1-year-old mice, including the accumulation of disaturated PC, further confirmation for a role for Lpla2 in surfactant degradation was based on the use of ESI/MS analysis of macrophages isolated from Lpla2 wild-type and null mice. These analyses revealed that of the measured lipids, PC and PE were most directly affected by the loss of Lpla2 activity. Those species of PC containing saturated fatty acids, most notably palmitate, as well as those with diacylglyceryl, plasmenyl, and plasmanyl linkages increased comparably in the absence of the acidic phospholipase A2 activity. These data suggest that Lpla2 does not discriminate among PCs with different aliphatic chains. By contrast, sphingomyelin and phosphatidic acid levels were not increased, consistent with the known substrate specificity of Lpla2.

A small change in ceramide content was observed. Lpla2 was originally identified as a 1-*O*-acylceramide synthase (3). This increase in ceramide may reflect the loss of this activity. However, the physiological role of Lpla2 as a regulator of ceramide metabolism remains to be clarified and is not obvious from the present study. Nevertheless, Lpla2 activity was measured in the wild-type and knockout mice using both ceramide and water as acceptors for the enzyme activity. By assaying Lpla2 as either a 1-*O*-acylceramide synthase or as a phospholipase A2, the enzyme activity was abolished to greater than 95% in the lungs and alveolar macrophages of the knockout mice, suggesting that Lpla2 represents the primary acidic phospholipase A2 activity found in lung.

ACKNOWLEDGMENTS

We gratefully acknowledge the technical assistance of Lisa Riggs for the preparation of the electron micrographs. We are grateful for helpful discussions with Kent Johnson on the interpretation of the alveolar macrophage ultrastructure. We are also grateful to Thom Saunders and Elizabeth Hughes for input on the vector design and transgenic animal studies.

REFERENCES

1. **Abe, A., M. Hiraoka, S. Wild, S. E. Wilcoxen, R. Paine III, and J. A. Shayman.** 2004. Lysosomal phospholipase A2 is selectively expressed in alveolar macrophages. J. Biol. Chem. **279:**42605–42611.
2. **Abe, A., and J. A. Shayman.** 1998. Purification and characterization of 1-O-acylceramide synthase, a novel phospholipase A2 with transacylase activity. J. Biol. Chem. **273:**8467–8474.
3. **Abe, A., J. A. Shayman, and N. S. Radin.** 1996. A novel enzyme that catalyzes the esterification of N-acetylsphingosine. Metabolism of C2-ceramides. J. Biol. Chem. **271:**14383–14389.
4. **Ames, G. F.** 1968. Lipids of *Salmonella typhimurium* and *Escherichia coli*: structure and metabolism. J. Bacteriol. **95:**833–843.
5. **Bligh, E. G., and W. J. Dyer.** 1959. A rapid method of total lipid extraction and purification. Can. J. Biochem. Physiol. **37:**911–917.
6. **Dranoff, G., A. D. Crawford, M. Sadelain, B. Ream, A. Rashid, R. T. Bronson, G. R. Dickersin, C. J. Bachurski, E. L. Mark, J. A. Whitsett, et al.** 1994.

Involvement of granulocyte-macrophage colony-stimulating factor in pulmonary homeostasis. Science **264:**713–716.
7. **Halliwell, W. H.** 1997. Cationic amphiphilic drug-induced phospholipidosis. Toxicol. Pathol. **25:**53–60.
8. **Han, X., and H. Cheng.** 2005. Characterization and direct quantitation of cerebroside molecular species from lipid extracts by shotgun lipidomics. J. Lipid Res. **46:**163–175.
9. **Han, X., and R. W. Gross.** 2005. Shotgun lipidomics: electrospray ionization mass spectrometric analysis and quantitation of cellular lipidomes directly from crude extracts of biological samples. Mass Spectrom. Rev. **24:**367–412.
10. **Han, X., and R. W. Gross.** 2005. Shotgun lipidomics: multidimensional MS analysis of cellular lipidomes. Expert Rev. Proteomics **2:**253–264.
11. **Han, X., J. Yang, H. Cheng, H. Ye, and R. W. Gross.** 2004. Toward fingerprinting cellular lipidomes directly from biological samples by two-dimensional electrospray ionization mass spectrometry. Anal. Biochem. **330:**317–331.
12. **Hiraoka, M., A. Abe, and J. A. Shayman.** 2002. Cloning and characterization of a lysosomal phospholipase A2, 1-O-acylceramide synthase. J. Biol. Chem. **277:**10090–10099.
13. **Mason, R. J., J. Nellenbogen, and J. A. Clements.** 1976. Isolation of disaturated phosphatidylcholine with osmium tetroxide. J. Lipid Res. **17:**281–284.
14. **Miles, P. R., L. Bowman, and M. J. Reasor.** 1996. Exposure to crystalline silica or treatment with chlorphentermine increases vitamin E levels in rat alveolar lavage materials. J. Toxicol. Environ. Health **49:**511–523.
15. **Noiriel, A., P. Benveniste, A. Banas, S. Stymne, and P. Bouvier-Nave.** 2004. Expression in yeast of a novel phospholipase A1 cDNA from Arabidopsis thaliana. Eur. J. Biochem. **271:**3752–3764.
16. **Reasor, M. J., and S. Kacew.** 2001. Drug-induced phospholipidosis: are there functional consequences? Exp. Biol. Med. (Maywood) **226:**825–830.
17. **Six, D. A., and E. A. Dennis.** 2000. The expanding superfamily of phospholipase A(2) enzymes: classification and characterization. Biochim. Biophys. Acta **1488:**1–19.
18. **Trapnell, B. C., J. A. Whitsett, and K. Nakata.** 2003. Pulmonary alveolar proteinosis. N. Engl. J. Med. **349:**2527–2539.